Published in final edited form as:
J Periodontol. 2011 July ; 82(7): 1007–1017. doi:10.1902/jop.2010.100577.

Gene Expression Dynamics During Bone Healing and Osseointegration

Zhao Lin[*], **Hector F. Rios**[†], **Sarah L. Volk**[†], **James V. Sugai**[†], **Qiming Jin**[†], and **William V. Giannobile**[†,‡]

[*]Division of Periodontology, Department of Oral Medicine, Infection and Immunity, Harvard School of Dental Medicine, Boston, MA; previously, Department of Periodontics and Oral Medicine, School of Dentistry, University of Michigan, Ann Arbor, MI

[†]Department of Periodontics and Oral Medicine, School of Dentistry, University of Michigan

[‡]Department of Biomedical Engineering, College of Engineering, University of Michigan

Abstract

Background—Understanding the molecular features of bone repair and osseointegration may aid in the development of therapeutics to improve implant outcomes. The purpose of this investigation is to determine the gene expression dynamics during alveolar bone repair and implant osseointegration.

Methods—An implant osseointegration preclinical animal model was used whereby maxillary defects were created at the time of oral implant placement, while a tooth extraction socket healing model was established on the contralateral side of each animal. The surrounding tissues in the zone of the healing defects were harvested during regeneration for temporal evaluation using histology, immunohistochemistry, laser capture microdissection, and quantitative reverse transcription–polymerase chain reaction for the identification of a panel of 17 putative genes associated with wound repair.

Results—In both models, three distinct expression patterns were displayed: 1) genes that are slowly increased during the healing process, such as bone morphogenetic protein 4, runt-related transcription factor 2, and osteocalcin; 2) genes that are upregulated at the early stage of healing and then downregulated at later stages, such as interleukin and chemokine (C-X-C motif) ligands 2 and 5; and 3) genes that are constitutively expressed over time, such as scleraxis. Although some similarities between osseointegration and tooth extraction socket were seen, distinct features developed and triggered a characteristic coordinated expression and orchestration of transcription factors, growth factors, extracellular matrix molecules, and chemokines.

Conclusions—Characterization of these events contributes to a better understanding of cooperative molecular dynamics in alveolar bone healing, and highlights potential pathways that could be further explored for the enhancement of osseous regenerative strategies.

Understanding important features of alveolar bone development, maturation, and repair has provided a wealth of information, lending insight toward promising therapeutic approaches that can bolster endogenous osseous regeneration in response to injury.[1–4] Currently, therapeutic approaches to enhance bone regenerative potential are available and continue to be optimized.[3,5–7] Identifying and understanding the dynamics of these important osteogenic environmental cues within alveolar socket healing and the osseointegration process are of

Correspondence: Dr. William V. Giannobile, Michigan Center for Oral Health Research, University of Michigan School of Dentistry, 1011 N. University Ave., Ann Arbor, MI 48109–1078. Fax: 734/763-5503;: william.giannobile@umich.edu.

critical importance. Greater knowledge about factors expressed during bone repair could serve as a foundation for novel therapeutic alternatives, addressing clinically challenging situations that often compromise the proper restoration of the bone's function and structure.[8]

The processes of alveolar tooth extraction socket healing and bone–implant osseointegration are similar in terms of bone healing, including such events as early protein expression, cell apposition, remodeling, and maturation of the healing site. At the microscopic level, the bone healing process starts with the formation of a coagulum, followed by infiltration of inflammatory cells that initiate removal of necrotic tissue. Subsequently, loose connective tissue migrates in and helps stabilize the extracellular matrix. This reparative fibrous connective tissue is eventually replaced by newly formed woven bone, and ultimately by lamellar bone and bone marrow.[9,10] At the molecular level, initial hematoma formation results in the release of platelet-derived growth factor, insulin-like growth factors, tumor-derived growth factor β, and fibroblast growth factors. These growth factors act as mitogenic and angiogenic signals at the early stage of bone healing. With the infiltration of connective tissue, the expression of bone morphogenetic proteins (BMPs) increases and osteogenesis is initiated.[11] Although extraction socket healing and osseointegration share many common aspects, they still have some differences: because of the trauma during osteotomy, the inflammatory response in osseointegration seems stronger than in the extraction socket healing site; and periodontal ligament (PDL) remnants may play a role in extraction socket healing, but PDL cells are not involved in osseointegration.

The biology of alveolar socket healing and implant osseointegration has been an area of intense research. However, because it is difficult to dissect the socket healing area from the alveolar bone for gene expression assay, most previous studies focus on histologic aspects of the healing process.[12–18] Very few investigations try to understand the dynamic gene expression profiles with emphasis on the spatial and temporal molecular characteristics.[19–22] Regarding osseointegration, although the gene expression profile of bone–titanium integration in long bone has been investigated by different methods, such as reverse transcription-polymerase chain reaction (RT-PCR) and microarray,[17,23] there is a scarcity of data regarding osseointegration dynamics in the oral cavity.

The purpose of this study is to determine the gene expression dynamics during alveolar bone healing and osseointegration. We used laser capture microdissection (LCM) to clearly dissect the tooth extraction healing region and implant osseointegration sites from alveolar ridge defects and identify gene expression profiles in a temporal fashion. The expression of a group of genes associated with osteogenesis, including growth factors, transcription factors, and chemokines, was examined and the results of selected gene markers were compared to bone reparative responses histologically. The knowledge obtained from this study should shed light on the design of future therapies for alveolar bone healing and osseointegration.

Materials and Methods

Experimental Design

Ethical board approval was obtained for this preclinical investigation by the University of Michigan, Unit for Laboratory Animal Medicine, Ann Arbor, Michigan. A total of ≈24 male Sprague–Dawley rats, 4 weeks of age, were used in this study.[§]The experimental timeline is shown in Figure 1. Animals were anesthetized under general anesthesia using ketamine (50 mg/kg) and xylazine (10 mg/kg) for the extractions and implant placements. Briefly, the first molars (M1) on one side of each maxilla were extracted. After 1 month, an osteotomy was performed at the residual ridge defects, and implants were placed as previously described.[24] Concurrent with implant placement, M1 teeth on the contralateral side of the maxillae were

extracted. In previous studies, ≈60% bone defect fill and 35% bone–implant contact were seen 14 days after implant placement.[24,25] To determine the gene expression profiles at early and late stages of healing, but prevent significant tissue damage while removing the implants, day 14 was selected as an endpoint. The animals were euthanized and the maxillae were dissected at 3, 7, 10, and 14 days after implant placement or tooth extraction. At each time point, Histologic evaluation including hematoxylin and eosin staining for tooth extraction and implant defect sites was performed on samples from six animals, followed by LCM, RNA extraction, and quantitative RT-PCR. Subsequently, immunohistochemistry staining was performed for selected genes (*Postn* and *Runx2*) to confirm the gene expression profiles.

Tooth Extraction, Defect Creation, Implant Placement

The surgical procedure is shown in Figure 1. Tooth extraction was performed by ZL, QJ, and HFR, and the implant placement was done by ZL and QJ. Briefly, the maxillary first molars (M1) were extracted using an atraumatic technique. The extraction sockets and soft tissues were allowed to heal for ≈30 days. After healing, an osteotomy was created using a custom drill as previously described.[24] The drill-bit was designed with a 0.95-mm diameter, 1-mm long apical portion and a 2.2-mm diameter, 1-mm long at the coronal aspect. The apical part of the drill created an osteotomy for initial fixation and the coronal part of the drill created a circumferential osseous defect before dental implant placement. The implants consisted of custom-fabricated, sterile, commercially pure, solid-cylinder titanium implants with a chemically modified surface by extensive hydroxylation/hydration with an average 4.1 to 4.7 μm roughness designed to the appropriate dimensions for placement into the rat maxillae (2 mm in length and 1 mm in diameter). The implants were press fit into position and evaluated for primary stability. The surgical field was closed by means of tissue glue.[¶] The animals were observed postoperatively on a heating pad until fully alert to ascertain their response to surgery. To maintain energy and prevent infection, animals were given a 10% dextrose solution containing 268 g/L ampicillin for 1 week post-surgery. A normal diet was continued for the animals.

Laser Capture Microdissection

The animals were sacrificed by CO_2 euthanasia at the designated time points after surgery. Block biopsies were harvested and immediately fixed with 10% phosphate-buffered neutral formalin for 24 hours. Biopsies were decalcified for 14 days in 10% EDTA solution. After implants were gently removed, biopsies were embedded in paraffin and cut sagittally along the axis of the tooth into 7-μm sections by microtome. LCM was performed to dissect out the areas of interest (see supplementary Fig. 1 in online *Journal of Periodontology*). Two different tissues from each animal were collected: osteotomy defect area and tooth extraction healing site. Demineralized tissue samples embedded in paraffin blocks were submitted to the University of Michigan Histology Core for sectioning. A total of three slides[#] containing three sections were cut for each sample block. The non-stained slides were then deparafinized by washing with xylene, two washes of 10 minutes per wash. The slides were air-dried. An LCM microscope[**] was used to cut the entire healing tooth extraction socket and peri-implant defect tissue. The tissues were collected into microcentrifuge tubes that contained RLT lysis buffer.[††] RNA was isolated using a kit.[‡‡]

Quantitative RT-PCR

Total RNA samples were extracted with a kit[§§] according to the manufacturer's instructions. [□□]RNA was subjected to RT in a 50-μL RT reaction using TaqMan RT reagents. cDNA was generated using random hexamer primers and oligo-T primers with 2:1 ratio. Subsequently, a preamplification kit was used to boost the low cDNA amount from LCM dissection.[¶¶] For quantitative real-time PCR, the generated cDNA was analyzed, in

triplicate, with a mix[##] in a sequence detection system.[***] The results were normalized with the 18S transcript. Primers and probes for *Bmp7*, wingless-type MMTV integration site family, member (*Wnt*) 4, 5A, 10b, CXCL5, transforming growth factor (*Tgf*)-*β1*, *Bmp4*, vascular endothelial growth factor (*Vegf*), interleukin (*Il*)-*1β*, *Cxcl2*, periostin (*Postn*), osteopontin (*Opn*), osteocalcin (*Ocn*), RUNX2, Lim domain mineralization protein (*Lmp1*), scleraxis (*Scx*), and *Cxcl12/Sdf1* were ordered from a manufacturer.[†††]

Immunohistochemistry

The specimens were dissected and fixed in 10% neutral buffered formalin at 4°C for 24 hours; demineralized in 10% EDTA solution over 3 weeks; dehydrated; embedded in paraffin; and processed for sectioning (6-μm thickness). Immunostaining of POSTN (ab14041, affinity purified rabbit polyclonal antibody)[‡‡‡] and RUNX2 (ab54868, mouse monoclonal)[§§§] was performed on paraffin sections using 1:8,000 and 1:1,000 primary antibody dilutions, respectively. Immunologic reactions were visualized by using an anti-rabbit HRP/DAB detection kit method (ab64261). □□□Bovine serum albumin 1% was used as a negative control. Sections were counterstained with hematoxylin and mounted on glass slides for analysis.

Statistical Analysis

Statistical analysis was performed using a software program.[¶¶¶] All data are presented as the mean ± SEM. The two-tailed analysis of variance statistical test was used to determine whether the differences in expression among groups were statistically significant at different time points. Bonferroni post hoc analysis of statistical significance was used to identify these differences. P values <0.05 were considered statistically significant.

Results

Descriptive Histology of Tooth Extraction Socket During Healing

Histologically, the extraction sockets followed a well-defined healing sequence (Fig. 2). At 3 days, large clots were seen in the sockets, surrounded by scattered neutrophils and a large amount of mesenchymal cells (severed PDL). At 7 days, the coagulum area condensed to a relatively small size, and more fibroblasts appeared in sockets. Newly formed bone, which is less stained, could be easily seen. At 10 days, clots were replaced by fibroblasts and new bone. At 14 days, the sockets were completely filled by new bone and bone marrow.

Descriptive Histology of Bone Healing and Osseointegration Around Dental Implants

Histologically, the healing after osteotomy was similar to extraction socket healing (Fig. 3). However, the healing appeared delayed with greater infiltration by inflammatory cells as seen in early stages. At the early stage (3 days), some blood clots were seen in the defect area. Few cells were found, and most of them were immune cells and scattered epithelial cells. By 7 days, the cell density in the defect area was higher and more extracellular matrix was seen. At 10 days, the defect site was mainly filled by fibroblasts. The border of the osteotomy site became less well defined, and newly formed bone started to grow into the defect area. At 14 days, more defect area was replaced by newly formed bone. Osseointegration could be observed during this stage.

Gene Expression Pattern of Tooth Extraction Socket Healing

We performed LCM to analyze the expression profile of genes associated with wound healing. We tested 17 genes, which can be categorized into three different groups: 1) growth factors and chemokines, 2) extracellular matrix proteins, and 3) transcription factors. Three expression patterns were evident (Fig. 4). The first pattern was genes that were slowly

increased during the healing process: growth factors (*Bmp4, Bmp7, Wnt10b, and Vegf*), transcription factors (*Runx2*), and extracellular matrix proteins related to mineralized tissue (*Opn and Ocn*) were in this group. Very interestingly, *Cxcl12 (Sdf1)* gradually increases during extraction socket healing. *Tgf-β1* increases at a mid-stage of healing (day 10) and then decreases. Similarly *Postn*, a target gene of *Tgf-β1*, had the same expression pattern. The second pattern was genes that were highly expressed at early time points and were downregulated at later stages. Chemokines *Il- 1β*, *Cxcl2, and Cxcl5*belonged to this category, although we did not see a statistical difference because of the limited number of animals. *Wnt5a*and *Wnt4* also seemed to decrease during healing. The final pattern was genes that were constitutively expressed. *Lmp1*, a scaffold protein that is involved in osteogenesis, and tendon-specific transcriptional factor *Scx* were in this group.

Gene Expression Pattern During Bone Regeneration Around Implants

The same 17 genes were also analyzed (Fig. 5). Interestingly, we were unable to detect some of the genes from osteotomy samples, such as *Bmp7*, *Wnt4*, *Wnt5a*, *Wnt10b*, and *Cxcl5*. The remaining genes followed a similar pattern as of extraction socket healing. Consistent with histologic images, at the early inflammation stage chemokines, such as *IL-1β* and *Cxcl2*, were highly expressed in the defect area and decreased at late time points. During healing, the expression of osteogenesis-related growth factors and chemokines (e.g., *Bmp4*, *Tgf-β1*, and *Cxcl12/Sdf1*) was gradually increased over time. Transcription factor *Runx2* followed the same trends. The expression of extracellular matrix proteins including *Opn*and *Postn* significantly increased at later stages (days 10 and 14). Interestingly, *Lmp1* gene expression was relatively high at day 3, but steadily decreased at later stages.

POSTN Protein Localization During Tooth Extraction Socket Healing

POSTN distribution within the healing socket clearly depicts areas of residual PDL structures around the wall of the alveolus at 3 days (Fig. 2). However, the proliferative granulation tissue that characterizes this healing stage presents minimal to no POSTN signal. By day 7, the sockets presented a denser connective tissue and a significant area was occupied by woven bone. The fibrous connective tissue present at this time point corresponded to an increased POSTN signal intensity. The POSTN distribution and localization among non-mineralized areas seems more homogeneous and intense by 10 days, but it seems to be present only within the less mature areas. This pattern seems to continue and by 14 days most of the socket is filled with mature trabecular bone, and therefore the POSTN signal is more localized and highlights isolated areas of greater bone metabolic activity.

POSTN Protein Localization During Bone Regeneration Around Implants

At 3 days, an inflammatory infiltrate seemed to dominate most of the area within the peri-implant defect and no POSTN signal was identified (Fig. 3). However, by 7 days a loose fibrous tissue has repopulated the peri-implant defect and distinct POSTN signal is visualized within the immature extracellular matrix. At 10 days a denser POSTN-positive connective tissue is clear together with an increasingly noticeable area of woven bone. Interestingly, at 14 days the mature trabecular structures are clearly surrounded by osteoblasts with no POSTN immunoreactivity. However, the immediately adjacent matrix and cellular population that localizes away from the bone surface presents an intense and well-defined signal.

RUNX2 Protein Localization During Tooth Extraction Socket Healing

The immunohistologic localization of RUNX2 at day 3 clearly shows a robust presence of RUNX2-positive cells within the granulation tissue that develops within the alveolar socket

(Fig. 2). By day 7 the RUNX2-expressing cells are localized mostly around and in close proximity to the immature mineralizing structures. At day 10 the positive immunoreactive cells are also localized within and aligned over the surface of the newly formed trabeculae. A clear increase in bone surface area characterizes the more mature alveolus and a corresponding saturation with RUNX2-positive cells.

RUNX2 Protein Localization During Bone Regeneration Around Implants

Contrary to the tooth extraction model, RUNX2 was not localized at 3 days within the peri-implant defect (Fig. 3). It was initially observed at 7 days within the loose connective tissue that was dominating the defect area. At 10 days a significant increase in signal and number of cells is clear and localizes primarily over the woven bone surface. At 14 days the matured structures are saturated within and over the surface by RUNX2-expressing cells.

Discussion

The physiology and biology of skeletal and alveolar bone are supported by a dynamic and complex milieu that ultimately determines structural and functional integrity.[26–32] In each one of these systems, multiple factors exert an effect (e.g., biochemical, hormonal, cellular, biomechanical) and collectively determine their quality.[33–37] Clinically, bone quality is perceived as an important feature that dictates the mechanical properties of bone over time. Within the skeleton, such characteristics vary from one area to another and are determined among many things by cellular density, connectivity, bone density, bone architecture, and the proportions of organic and inorganic matrix.[34,38–41] These characteristics are the result of the orchestration of growth factors (e.g., *Bmps*, *Vegf*, and *Tgfβ-1*); matrix molecules (e.g., *Opn*, *OCN*, and*POSTN*); immunologic mediators and cytokines (e.g., *Il1-β*, *Cxcl-2, -5* and *-12*); and the action of important transcription factors and intracellular molecules overtime (e.g., *Runx2, Lmp1, and Scx*).

This physiologic balance is often disrupted abruptly after an injury. Therefore, healing of an injured tissue usually leads to the formation of a tissue that differs in morphology or function from the original tissue. This type of healing is called “repair.” Although, it may contain similar environmental cues that lead the osteogenic process, the spatial and temporal dynamics of the molecules may lean toward a delayed or altered healing.[42–45] Tissue “regeneration,” however, is a term used to describe a healing process that leads to complete restoration of morphology and function. Therefore, the success of bone regeneration and osseointegration is influenced by an understanding of the basic biologic and physiologic principles of bone, because it aids the surgeon in selecting appropriate biologics to enhance alveolar bone homeostasis.[46–48]

Capturing the molecular dynamic events that occur during healing both in a socket healing and implant osseointegration process represents a first step toward understanding the cooperative action of multiple factors including growth factors, extracellular matrix molecules, and chemokines. Wound healing therapeutic methods using growth factors to target restoration of alveolar bone has advanced the field of oral and periodontal regenerative medicine.[49,50] A major focus of oral and craniofacial reconstruction is on the impact of growth factor delivery strategies using growth factor–producing cells, proteins, or genes encoding growth factors.[49] Advances in molecular cloning have made available unlimited quantities of recombinant growth factors for applications in tissue engineering of the craniofacial complex including alveolar bone. Within the alveolar socket and peri-implant space several interactions between cells and a diverse mixture of matrix proteins take place.

We noted for both the bone repair model and the osseointegration models that three distinct expression patterns were displayed (Figs. 4 and 5). The first pattern is genes that are slowly increased during the healing process, such as *Bmp4, Runx2, and Ocn*. These genes are well-known to be critical in the early stages of osteogenesis and bone regeneration.[51] The second pattern included genes that are upregulated at the early stage of healing and then downregulated at later stages, such as *Il-1β*, *Cxcl2, and Cxcl5*.[52] These molecules may indeed be of significant importance in the host defense during the early stages of inflammation and soft tissue wound repair. The final pattern is genes that are constitutively expressed overtime, such as *Scx* (e.g., *Scx* is a member of the basic-helix-loop-helix superfamily of transcription factors).[53] As such, cells in the healing wound site may lead to the eventual formation of tendon tissue, which may provide particular progenitors of connective and ligamentous tissues.

Within the scope of this study, we selected POSTN and RUNX2 protein localization to show the events that mediate both matrix stabilization and cell maturity. In future studies, dynamics with respect to the protein dynamics for other important matrix molecules, growth factors, and transcription factors should be explored. Particularly interesting is the exclusive spatial expression of POSTN by remnants of the PDL on the healing socket at 3 days. This distinct expression pattern contrasts with its absence within the rapidly proliferative granulation tissue. Interestingly, a significant number of RUNX2-positive cells seemed to populate and dominate the clot and supportive connective tissue. As the healing process evolves, both POSTN and RUNX2 expression increases spatially within the healing area as reflected at 7 days. By 10 days, the protein localization polarizes primarily to the bone surface area in the case of RUNX2, and POSTN is limited to areas that appeared less matured but with intense signal. This pattern is maintained and even more distinct as the tissue matures, as shown by 14 days.

Similarly to the tooth extraction model, the peri-implant healing process mimics the dynamics of the healing alveolus. However, the early events at 7 and 10 days are delayed and reflect a less mature healing environment. POSTN distribution is clearly limited to the preosteoblastic supportive connective tissue, whereas RUNX2 is more intense within osteocytic and osteoblastic cells.

Although bone tissue exhibits a large regeneration potential and may restore its original structure and function completely, bony defects may often fail to heal properly. Identifying critical aspects that stabilize the wound and mediate the osteogenic process could help favor healing in osseous defects in challenging clinical situations. These data together with the current developments in cell, protein, and gene delivery technology offer exciting potential therapeutic pathways to aid the clinician in the predictable repair of bone defects to allow oral reconstructive therapies for patient care.

Conclusions

Overall, the expression of osteogenesis-related growth factors was gradually increased over time, whereas chemokines tended to decrease. The expression of extracellular matrix proteins significantly increased at later stages (days 10 and 14). There was an apparent tissue maturation delayed during osseointegration, compared to the alveolar socket healing or what could be interpreted as an extended maturation phase. Future investigations can hopefully extend on this work to better understand the molecular mechanisms of oral bone repair and osseointegration.

Supplementary Material

Refer to Web version on PubMed Central for supplementary material.

Acknowledgments

The authors thank Chris Jung, Department of Periodontics and Oral Medicine, University of Michigan, for assisting with the preparation of the figures. They also thank Christopher Strayhorn, Department of Periodontics and Oral Medicine, University of Michigan, for performing the histologic sectioning. They acknowledge the technical contributions of Mallory Mitchell and Min Oh, Department of Periodontics and Oral Medicine, University of Michigan. This work was supported by the ITI Foundation (WVG), NIH Grant DE13397 (WVG), and 1K23DE019872 (HFR). ZL was also supported by the Predoctoral Fellowship from Rackham Graduate School at the University of Michigan. The authors report no conflicts of interest related to this study.

References

1. Panetta NJ, Gupta DM, Longaker MT. Bone regeneration and repair. Curr Stem Cell Res Ther. 2010; 5:122–128. [PubMed: 19941457]
2. Gersbach CA, Phillips JE, García AJ. Genetic engineering for skeletal regenerative medicine. Annu Rev Biomed Eng. 2007; 9:87–119. [PubMed: 17425467]
3. Kimelman N, Pelled G, Helm GA, Huard J, Schwarz EM, Gazit D. Review: Gene- and stem cell-based therapeutics for bone regeneration and repair. Tissue Eng. 2007; 13:1135–1150. [PubMed: 17516852]
4. Secreto FJ, Hoeppner LH, Westendorf JJ. Wnt signaling during fracture repair. Curr Osteoporos Rep. 2009; 7:64–69. [PubMed: 19631031]
5. Lee J, Stavropoulos A, Susin C, Wikesjö UM. Periodontal regeneration: Focus on growth and differentiation factors. Dent Clin North Am. 2010; 54:93–111. [PubMed: 20103474]
6. Mahendra A, Maclean AD. Available biological treatments for complex non-unions. Injury. 2007; 38(Suppl 4):S7–S12. [PubMed: 18224732]
7. Schmidmaier G, Schwabe P, Strobel C, Wildemann B. Carrier systems and application of growth factors in orthopaedics. Injury. 2008; 39(Suppl 2):S37–S43. [PubMed: 18804572]
8. Schilephake H. Bone growth factors in maxillofacial skeletal reconstruction. Int J Oral Maxillofac Surg. 2002; 31:469–484. [PubMed: 12418561]
9. Cardaropoli G, Araújo M, Lindhe J. Dynamics of bone tissue formation in tooth extraction sites. An experimental study in dogs. J Clin Periodontol. 2003; 30:809–818. [PubMed: 12956657]
10. Berglundh T, Abrahamsson I, Lang NP, Lindhe J. De novo alveolar bone formation adjacent to endosseous implants. Clin Oral Implants Res. 2003; 14:251–262. [PubMed: 12755774]
11. Franceschi RT. Biological approaches to bone regeneration by gene therapy. J Dent Res. 2005; 84:1093–1103. [PubMed: 16304438]
12. Amler MH, Johnson PL, Salman I. Histological and histochemical investigation of human alveolar socket healing in undisturbed extraction wounds. J Am Dent Assoc. 1960; 61:32–44. [PubMed: 13793201]
13. Amler MH. The time sequence of tissue regeneration in human extraction wounds. Oral Surg Oral Med Oral Pathol. 1969; 27:309–318. [PubMed: 5251474]
14. Lin WL, McCulloch CA, Cho MI. Differentiation of periodontal ligament fibroblasts into osteoblasts during socket healing after tooth extraction in the rat. Anat Rec. 1994; 240:492–506. [PubMed: 7879901]
15. Kuboki Y, Hashimoto F, Ishibashi K. Time–dependent changes of collagen crosslinks in the socket after tooth extraction in rabbits. J Dent Res. 1988; 67:944–948. [PubMed: 3170907]
16. Kojima N, Ozawa S, Miyata Y, Hasegawa H, Tanaka Y, Ogawa T. High–throughput gene expression analysis in bone healing around titanium implants by DNA microarray. Clin Oral Implants Res. 2008; 19:173–181. [PubMed: 18184341]
17. Ogawa T, Nishimura I. Genes differentially expressed in titanium implant healing. J Dent Res. 2006; 85:566–570. [PubMed: 16723657]

18. Joos U, Wiesmann HP, Szuwart T, Meyer U. Mineralization at the interface of implants. Int J Oral Maxillofac Surg. 2006; 35:783–790. [PubMed: 16697141]
19. Sukotjo C, Abanmy AA, Ogawa T, Nishimura I. Molecular cloning of wound inducible transcript (wit 3. 0) differentially expressed in edentulous oral mucosa undergoing tooth extraction wound-healing. J Dent Res. 2002; 81:229–235. [PubMed: 12097305]
20. Karimbux NY, Sirakian A, Weber HP, Nishimura I. A new animal model for molecular biological analysis of the implant-tissue interface: Spatial expression of type XII collagen mRNA around a titanium oral implant. J Oral Implantol. 1995; 21:107–113. discussion 114–105. [PubMed: 8699501]
21. Shyng YC, Devlin H, Riccardi D, Sloan P. Expression of cartilage-derived retinoic acid-sensitive protein during healing of the rat tooth-extraction socket. Arch Oral Biol. 1999; 44:751–757. [PubMed: 10471159]
22. Devlin H, Sloan P. Early bone healing events in the human extraction socket. Int J Oral Maxillofac Surg. 2002; 31:641–645. [PubMed: 12521322]
23. Omar O, Svensson S, Zoric N, et al. In vivo gene expression in response to anodically oxidized versus machined titanium implants. J Biomed Mater Res A. 2010; 92:1552–1566. [PubMed: 19431206]
24. Chang PC, Seol YJ, Cirelli JA, et al. PDGF-B gene therapy accelerates bone engineering and oral implant osseointegration. Gene Ther. 2010; 17:95–104. [PubMed: 19741730]
25. Chang PC, Seol YJ, Kikuchi N, Goldstein SA, Giannobile WV. Functional apparent moduli as predictors of oral implant osseointegration dynamics. J Biomed Mater Res B Appl Biomater. 2010; 94:118–126. [PubMed: 20524185]
26. Bonewald LF, Johnson ML. Osteocytes, mechanosensing and Wnt signaling. Bone. 2008; 42:606–615. [PubMed: 18280232]
27. Burger EH, Klein-Nulend J, van der Plas A, Nijweide PJ. Function of osteocytes in bone—Their role in mechanotransduction. J Nutr. 1995; 125(Suppl 7):2020S–2023S. [PubMed: 7602386]
28. Duncan RL, Turner CH. Mechanotransduction and the functional response of bone to mechanical strain. Calcif Tissue Int. 1995; 57:344–358. [PubMed: 8564797]
29. Marotti G. The osteocyte as a wiring transmission system. J Musculoskelet Neuronal Interact. 2000; 1:133–136. [PubMed: 15758506]
30. Marotti G, Palumbo C. The mechanism of transduction of mechanical strains into biological signals at the bone cellular level. Eur J Histochem. 2007; 51(Suppl 1):15–19. [PubMed: 17703589]
31. Rios H, Koushik SV, Wang H, et al. Periostin null mice exhibit dwarfism, incisor enamel defects, and an early-onset periodontal disease-like phenotype. Mol Cell Biol. 2005; 25:11131–11144. [PubMed: 16314533]
32. Rios HF, Ma D, Xie Y, et al. Periostin is essential for the integrity and function of the periodontal ligament during occlusal loading in mice. J Periodontol. 2008; 79:1480–1490. [PubMed: 18672999]
33. Fortunati D, Reppe S, Fjeldheim AK, Nielsen M, Gautvik VT, Gautvik KM. Periostin is a collagen associated bone matrix protein regulated by parathyroid hormone. Matrix Biol. 2010; 29:594–601. [PubMed: 20654714]
34. Ammann P, Rizzoli R. Bone strength and its determinants. Osteoporos Int. 2003; 14(Suppl 3):S13–S18. [PubMed: 12730800]
35. Ma YL, Dai RC, Sheng ZF, et al. Quantitative associations between osteocyte density and biomechanics, microcrack and microstructure in OVX rats vertebral trabeculae. J Biomech. 2008; 41:1324–1332. [PubMed: 18342320]
36. Havens AM, Chiu E, Taba M, et al. Stromal-derived factor-1alpha (CXCL12) levels increase in periodontal disease. J Periodontol. 2008; 79:845–853. [PubMed: 18454663]
37. Wallach S, Farley JR, Baylink DJ, Brenner-Gati L. Effects of calcitonin on bone quality and osteoblastic function. Calcif Tissue Int. 1993; 52:335–339. [PubMed: 8504368]
38. Dalle Carbonare L, Giannini S. Bone microarchitecture as an important determinant of bone strength. J Endocrinol Invest. 2004; 27:99–105. [PubMed: 15053252]

39. Jin Q, Wei G, Lin Z, et al. Nanofibrous scaffolds incorporating PDGF-BB microspheres induce chemokine expression and tissue neogenesis in vivo. PLoS One. 2008; 3:e1729. [PubMed: 18320048]
40. O'Brien FJ, Brennan O, Kennedy OD, Lee TC. Microcracks in cortical bone: How do they affect bone biology? Curr Osteoporos Rep. 2005; 3:39–45. [PubMed: 16036100]
41. Viguet-Carrin S, Garnero P, Delmas PD. The role of collagen in bone strength. Osteoporos Int. 2006; 17:319–336. [PubMed: 16341622]
42. Hu D, Lu C, Sapozhnikova A, et al. Absence of beta3 integrin accelerates early skeletal repair. J Orthop Res. 2010; 28:32–37. [PubMed: 19637214]
43. Kwong FN, Hoyland JA, Freemont AJ, Evans CH. Altered relative expression of BMPs and BMP inhibitors in cartilaginous areas of human fractures progressing towards nonunion. J Orthop Res. 2009; 27:752–757. [PubMed: 19058174]
44. Weiss S, Zimmermann G, Pufe T, Varoga D, Henle P. The systemic angiogenic response during bone healing. Arch Orthop Trauma Surg. 2009; 129:989–997. [PubMed: 19037648]
45. Szczesny G, Olszewski WL, Zagozda M, et al. Genetic factors responsible for long bone fractures non-union. Arch Orthop Trauma Surg. 2010 Aug 21.
46. Einhorn TA. The Wnt signaling pathway as a potential target for therapies to enhance bone repair. Sci Transl Med. 2010; 2:42ps36.
47. Minear S, Leucht P, Jiang J, et al. Wnt proteins promote bone regeneration. Sci Transl Med. 2010; 2:29ra30.
48. Chen Y, Whetstone HC, Lin AC, et al. Beta-catenin signaling plays a disparate role in different phases of fracture repair: Implications for therapy to improve bone healing. PLoS Med. 2007; 4:e249. [PubMed: 17676991]
49. Kaigler D, Cirelli JA, Giannobile WV. Growth factor delivery for oral and periodontal tissue engineering. Expert Opin Drug Deliv. 2006; 3:647–662. [PubMed: 16948560]
50. Ramseier CA, Abramson ZR, Jin Q, Giannobile WV. Gene therapeutics for periodontal regenerative medicine. Dent Clin North Am. 2006; 50:245–263. ix. [PubMed: 16530061]
51. Zaky SH, Cancedda R. Engineering craniofacial structures: Facing the challenge. J Dent Res. 2009; 88:1077–1091. [PubMed: 19897785]
52. De Donatis A, Ranaldi F, Cirri P. Reciprocal control of cell proliferation and migration. Cell Commun Signal. 2010; 7(8):20. [PubMed: 20822514]
53. Noda M, Nifuji A, Tuji K, et al. Transcription factors and osteoblasts. Front Biosci. 1998; 3:d817–d820. [PubMed: 9682037]

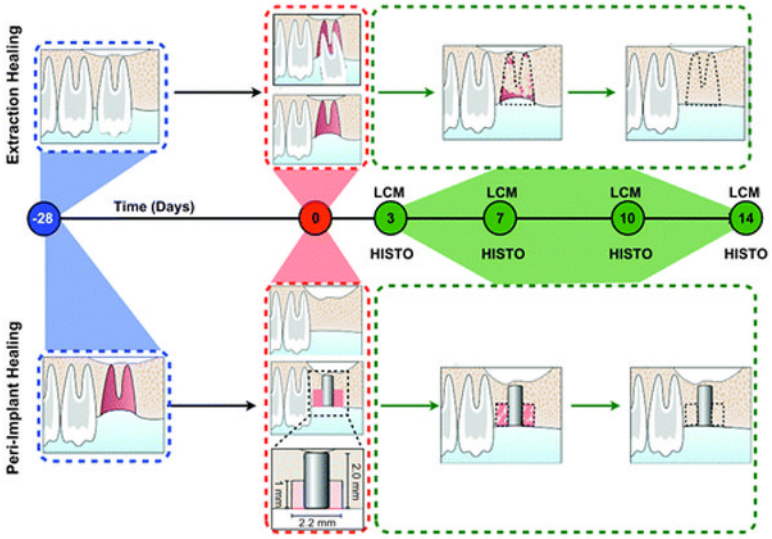

Figure 1.

Alveolar socket and peri-implant defect healing study models and timeline. The top and bottom panels represent the sequence of events that characterize the extraction and peri-implant healing models, respectively. The left first maxillary molar (M1) was extracted and allowed to completely heal for 28 days. On the healed ridge, an implant osteotomy was created that allowed implant placement and creation of a standardized peri-implant defect. In the contralateral side, M1 was extracted. LCM and histology (HISTO) methods were used for the analysis and evaluation of the healing area (black dotted line) at days 3, 7, 10, and 14.

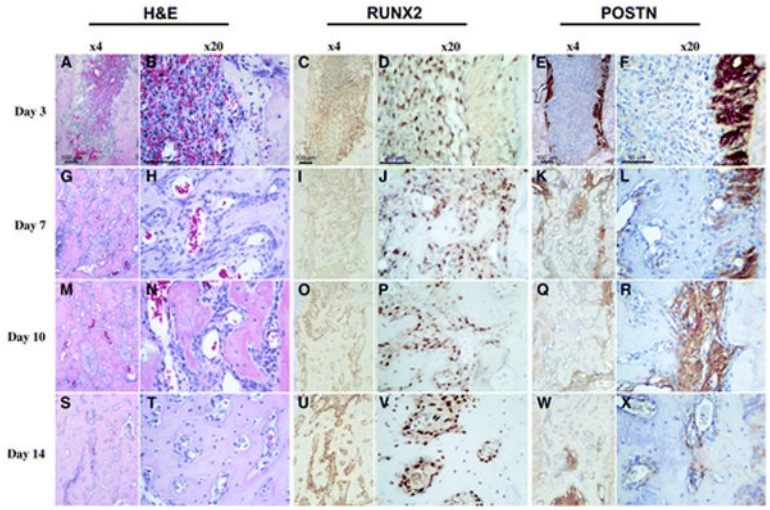

Figure 2.

Histologic evaluation of alveolar socket healing sites over time. Hematoxylin and eosin (H&E), RUNX2, and POSTN immunohistochemistry for tooth extraction site healing at 3, 7, 10, and 14 days (left panels, original magnification ×4; right panels, original magnification ×20). **A** and **B)** A clearly visible blood clot is noticeable at day 3. **C** and **D)** A significant number of RUNX2-positive cells are noticed within the alveolar socket populating the clot. **E**and **F)** Remnants of the periodontal ligament can be clearly depicted by its strong POSTN staining at day 3. **G through L)** At day 7, the cell density in the defect area is higher and the POSTN- and RUNX2-positive cells start colocalizing within these areas. **M through R)** At day 10, the defect site seems to be filled by a condensed mesenchymal tissue. **S through X)** Finally, by day 14, an integration of the newly formed bone to the original socket walls is noticed.

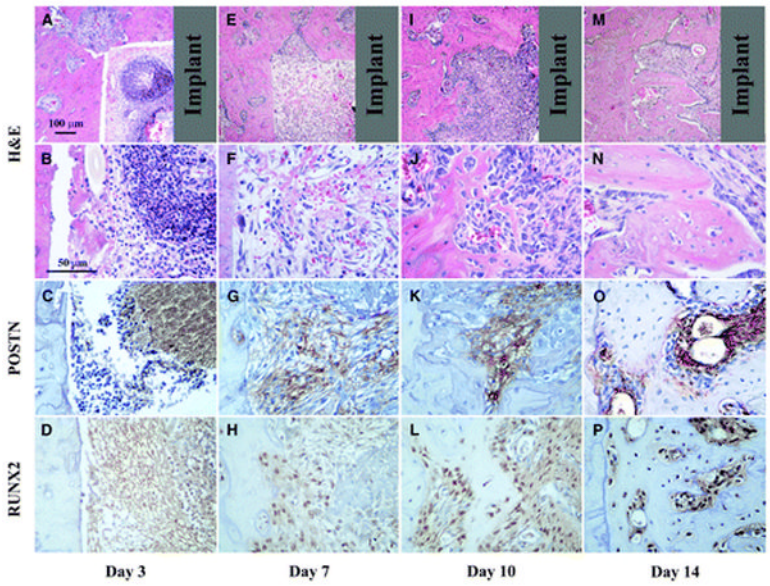

Figure 3.

Healing response for peri-implant repair sites at 3, 7, 10, and 14 days. **A through D)** Initially, inflammatory cells seem to dominate the defect area as depicted at day 3. **E through H)** By day 7, a loose fibrous connective tissue fills the defect and clear POSTN and RUNX2 staining is present. **I through L)** At day 10, RUNX2-positive cells are abundant and POSTN is gradually limited to the more immature tissue areas. **M through P)** Similar to the tooth extraction healing sites, at day 14, an integration of the newly formed bone to the walls of the defect is clear. Gray color in the top panels represents the implant location area (top panels, original magnification ×4; second, third, and fourth panels and rows, original magnification ×20).

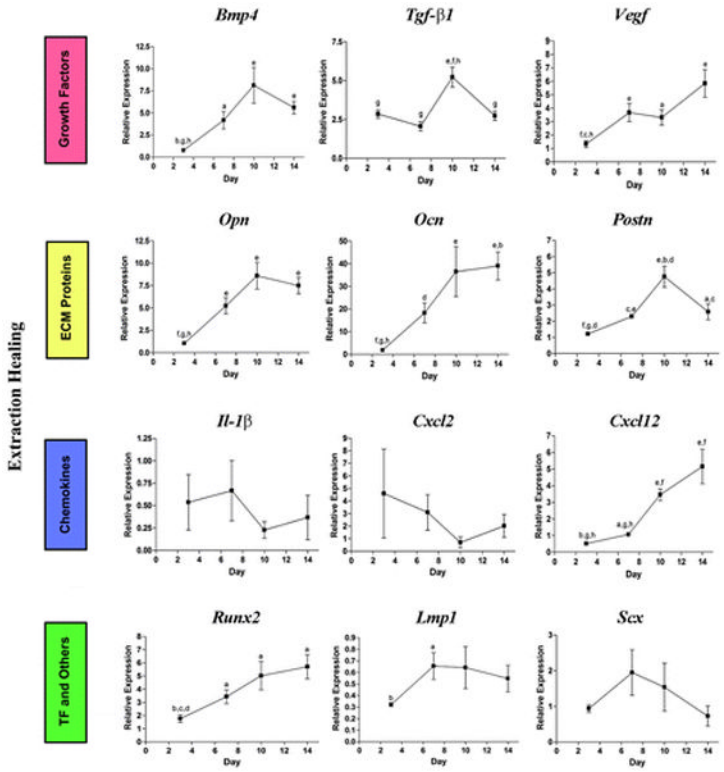

Figure 4.

Gene expression pattern of tooth extraction socket healing sites. ECM = extracellular matrix; TF = transcription factors. a = $P<0.05$ compared to day 3; b= $P<0.05$ compared to day 7; c = $P<0.05$ compared to day 10; d = $P<0.05$ compared to day 14; e = $P<0.01$ compared to day 3; f = $P<0.01$ compared to day 7; g = $P<0.01$ compared to day 10; h = $P<0.01$ compared to day 14.

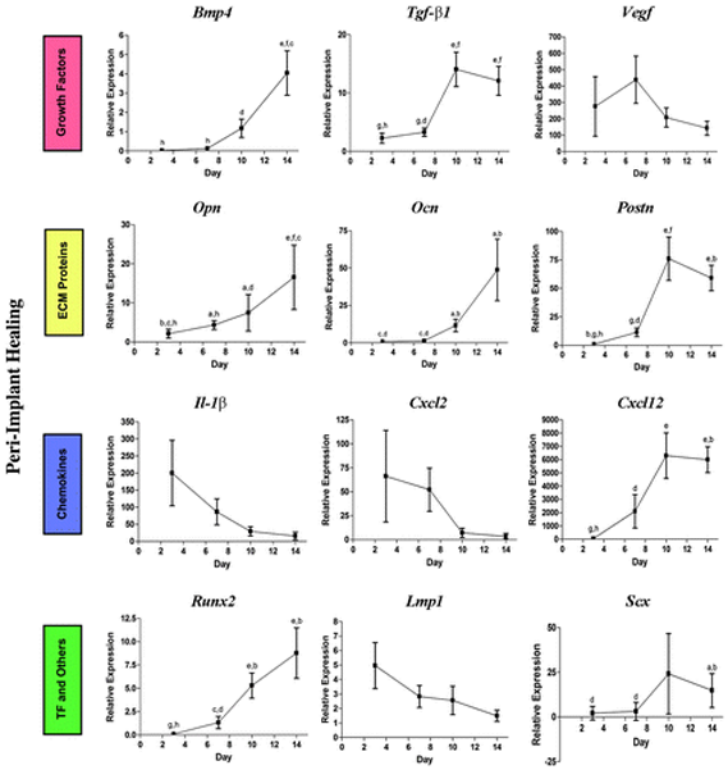

Figure 5.

Gene expression pattern of bone regenerative sites around implants. ECM = extracellular matrix; TF = transcription factors. a = $P<0.05$ compared to day 3; b = $P<0.05$ compared to day 7; c = $P<0.05$ compared to day 10; d = $P<0.05$ compared to day 14; e = $P<0.01$ compared to day 3; f = $P<0.01$ compared to day 7; g = $P<0.01$ compared to day 10; h = $P<0.01$ compared to day 14.